



Synthesis of Triazatruxene-Based Derivatives for Optoelectronic Applications

Shivanshu Tripathi^{1*}, Kusum Yadav², Varsha Nigam Gour¹

¹Department of Chemistry, Sanjeev Agrawal Global Education (SAGE) University, Bhopal, Madhya Pradesh, India

²Senior Research Fellow, Indian Institute of Technology, Indore, Madhya Pradesh, India

Article History

Received on: 11/08/2024

Revised on: 27/08/2024

Accepted on: 31/08/2024

Published on: 17/09/2024

Keywords

Triazatruxene

Photophysical

Electrochemical

Thermally Activated

Fluorescence

ABSTRACT

Recently, triazatruxene-based molecules have shown excellent efficiency for thermally activated delayed fluorescence (TADF) organic light emitting diodes (OLEDs) and hole transporting materials (HTMs) for perovskite solar cells. We have synthesized the donor moiety triazatruxene (TAT) and its three derivatives TAT-Alk, TAT-Alk-Br and TAT-Alk-3Br by alkylation and bromination of TAT. Photophysical and electrochemical studies were carried out to explore its optoelectronic applications.

*Corresponding Author

Mr. Shivanshu Tripathi
Email: tripathi130320@gmail.com

Scan QR to visit website



JOURNAL OF PHARMACOLOGY AND BIOMEDICINE

ISSN No. 2456-8244

Publication Hosted by
jpbiomed.com

Introduction

In 1965, Baars *et al.* successfully synthesized triazatruxene (TAT) for the first time by reacting indole with formaldehyde using a Lewis acid catalyst. This innovative achievement laid the groundwork for further investigation into TAT derivatives and their possible uses, especially in organic electronics and optoelectronics. Building on this initial synthesis, recent studies have explored the different properties of TAT-based materials, revealing their prominent solubility, thermal stability, and electronic features, which make them highly appropriate for a range of advanced technological applications.^[1-3]



Triazatruxene (TAT) based discotic liquid crystals (DLCs) hold great potential for semiconductor applications because of their disc-shaped structure, which favors the formation of well-ordered columnar phases that improve charge transport productivity. Noted for their ability to self-assemble and their thermal stability, TAT-based DLCs create uniform columnar structures that are essential for reliable charge mobility in devices such as organic light-emitting diodes (OLEDs) and organic photovoltaic cells (OPVs). This consistent structural arrangement enhances the implementation of semiconductor devices by providing stable pathways for charge transport.^[4-5]

Researchers have utilized a unique methodology known as single crystal X-ray diffraction to investigate the crystal structures of TAT derivatives. This study provides insights into the interactions between these molecules and their formation of columnar structures.

Triazatruxene derivatives have been studied for their potential use as Hole Transport Materials (HTMs) in Perovskite Solar Cells (PSCs) because of their beneficent electronic properties and stability. In particular, HTMs based on triazatruxene have substantiated encouraging outcomes in improving both the efficiency and stability of PSCs^[6].

Thermally activated delayed fluorescence (TADF) materials play an important role to making OLEDs highly efficient because as they enable the achievement of 100% internal quantum efficiency (IQE)^[8].

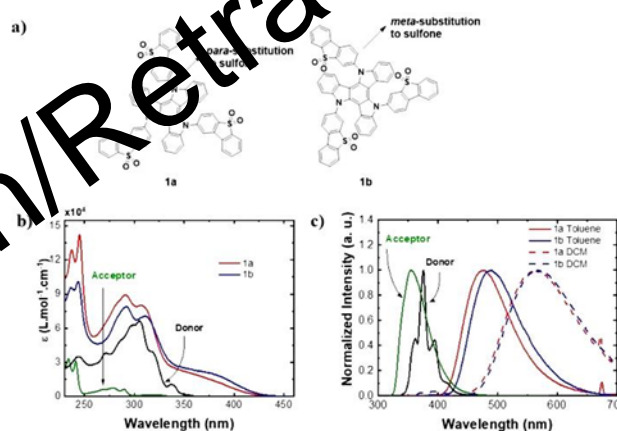


Figure 1 (a) Chemical structure of para-substituted emitter (1a) and meta-substituted emitter (1b), (b) extinction coefficient absorption spectra of the acceptor (A) and donor (D) Ref. 10.1002/eptc.202200248

These materials are good at transforming non-light-emitting triplet states into light-emitting singlet states, thereby enhancing the overall external quantum efficiency of OLEDs. Recent research has focused on optimizing these ma-

materials through punctilious design, leading to produce various colors and improve device performance.^[7]

The triazatruxene derivatives demonstrate strong potential as selective G-quadruplex ligands, justifying further study of their biological activity. Their supremacy water solubility and DNA binding properties indicate enhancing pharmacological effects, especially in the inhibition of tumor cell growth; place them as promising candidates for future studies.^[9]

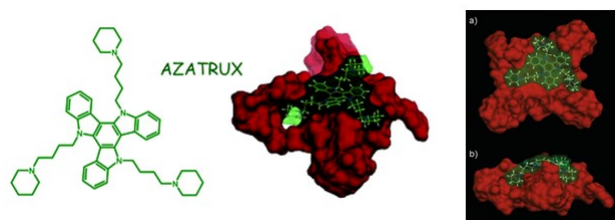


Figure 2 Complex of AZATRUX Ref. 10.1039/B904723A

In **Figure 2**, complex of AZATRUX (stick model with yellow transparent surface) with the human monomeric G-quadruplex DNA (red surface), obtained by simulated annealing, (a) top view, (b) lateral view.^[9]

In this study, we have successfully synthesized triazatruxene (TAT) and its derivatives **TAT**, **TAT-Alk**, **TAT-Alk-Br**, and **TAT-Alk-3Br**. These compounds were characterized using LCMS, HRMS, ¹H & ¹³C NMR techniques. Our primary objective is to investigate the photo-physical and electrochemical of these synthesized molecules.

In 2021, Zhou *et al.*, presented the development of two star-shaped TADF emitters, **TATC-TRZ** and **TATP-TRZ**, with distinct side chains. Both emitters exhibited comparable photo physical properties and TADF characteristics. Notably, the flexible alkyl chain in TATC-TRZ significantly enhances film formation and

stability, leading to superior device performance. Consequently, TATC-TRZ-based OLEDs achieved markedly higher efficiencies (EQE_{max} of 7.5% and CE_{max} of 19.9 cd/A) than TATP-TRZ-based OLEDs (EQE_{max} of 2.8% and CE_{max} of 7.4 cd/A), highlighting the efficacy of flexible alkyl tails in improving solution-processed devices.^[10]

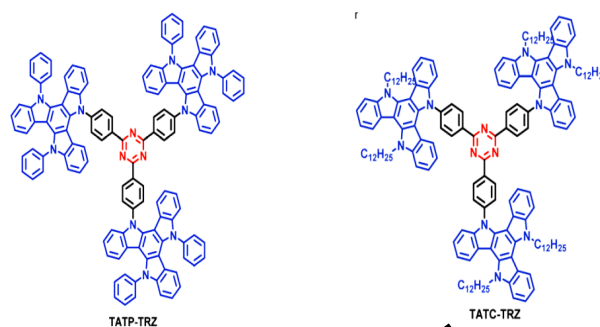


Figure 3 Designed molecules of TATP-TRZ & TATC-TRZ

In 2021, Aslan *et al.*, have successfully synthesized arylated-triazatruxene motifs at the **C1**, **C6**, and **C11** positions through a functionalization/cyclotrimerization process, influenced significantly by the nature of substituents at non-peripheral positions of oxindoles. This method is operationally simple, broad in substrate scope, and scalable, hence providing a practical route to functionalized triazatruxene derivatives. We also demonstrated the synthesis of a new type-two atropisomer for oxindole and triazatruxene. Notably, the triazatruxene scaffold 9a showed potential in OLED technology when used as an emitting layer in a white OLED device. Future efforts will focus on extending the synthetic functionalization of triazatruxene and enhancing their OLED performance, considering the commercialization.^[11]

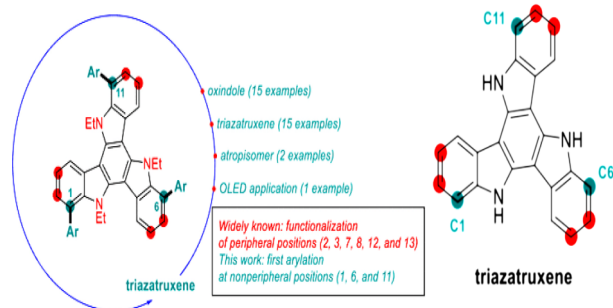


Figure 4 Structure of triazatruxene based arylation at nonperipheral positions (1, 6 and 11)

Recently, researchers have synthesized three novel bridged triazatruxene derivatives named **1FTAT-2Ph**, **2FTAT-1Ph**, **3FTAT**, as solution-processed host materials for TADF OLEDs, featuring diphenyl methylene bridging groups that enhance molecular rigidity, thermal stability, and high T1 energy levels (~ 2.8 eV). The 2FTAT-1Ph based device achieved the best performance with a maximum EQE of **20.9** and a maximum PE of **72.7 lm/W**, showing balanced charge transport and high QY in the EML (Emitter layer). The elevated HOMO levels of bridged triazatruxene derivatives matched well with the Fermi level of the ITO/PEDOT anode, improving hole injection and transport. This resulted in a power efficiency of **72.7 lm/W**, much higher than the **36.1 lm/W** of the classical CBP host-based devices, showcasing a new strategy for high-performance solution-processed TADF OLEDs. [12, 13, 14]

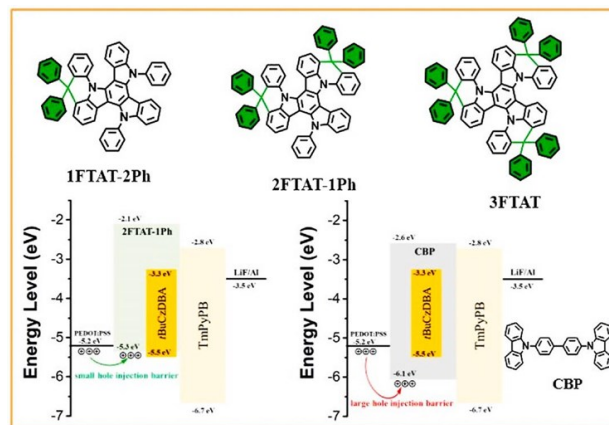
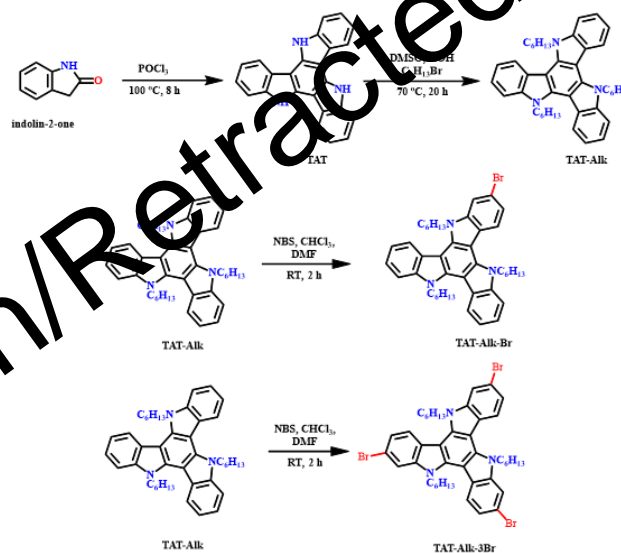


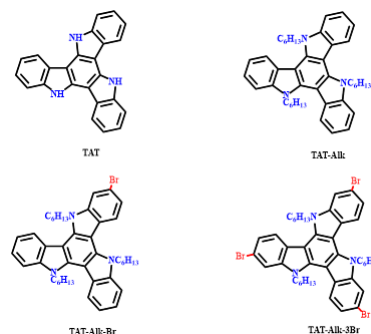
Figure 5 Comparison of the device energy level diagrams with 2FTAT-1Ph and CBP as host.

Material and Methods

The pathway of synthesizing the desired compounds is presented in Scheme 1 and the structures of the synthesized derivatives is presented in Scheme 2.



Scheme 1 Synthetic route to TAT, TAT-Alk, TAT-Alk-Br, TAT-Alk-3Br



Scheme 2 Synthesized molecules

The following procedures were adopted for the preparation of the compounds **TAT**, **TAT-Alk**, **TAT-Alk-Br**, and **TAT-Alk-3Br**.

Synthesis of compound Triazatruxene (TAT):

A mixture of 2-oxindolinone (6g, 45.06 mmol) and POCl₃ (30 mL) was heated at 100 °C for 8h. The cooled reaction mixture was slowly poured into crushed ice water and the mixture was neutralized carefully with a saturated KOH solution added in small quantities. After neutralization, the precipitate was filtered to give the crude product as a brown solid. The obtained crude product was purified by column chromatography (Hexane:Acetone = 90:10 vol/vol). After evaporation of the solvent at reduced pressure and recrystallization from acetone, the compound **TAT** was obtained as an off white solid (2g, 38% yield). **¹H NMR** (500MHz, DMSO -d₆) δ = 11.87 (s, 3 H), 8.68 (d, *J* = 7.6 Hz, 3 H), 7.73 (d, *J* = 7.8 Hz, 3 H), 7.42 - 7.38 (m, 3 H), 7.36 - 7.32 (m, 3 H), **¹³C NMR** (125 MHz, DMSO -d₆) δ = 139.0, 134.3, 122.9, 122.7, 120.3, 119.6, 111.4, 101.0. **LCMS** (ESI) *m/z* calcd for C₂₄H₁₅N₃: 345.1260, [M] Found: 345.1217.

Synthesis of compound Alkylated-TAT

TAT (2.4 g, 6.65 mmol) was dissolved in dry DMSO (30 mL) under an argon atmosphere and treated under vigorous stirring with KOH (4.48 g, 79.9 mmol) at 70 °C, after 1 h 1-bromohexane (5.63 mL, 9.95 mmol) was added. After 18 h the reaction mixture, taken up in ethyl acetate, and dried under reduced pressure to give the crude product as black solid. The obtained crude product was purified by column chromatography (Hexane:DCM = 95:5 vol/vol). After evaporation of the solvent at reduced pressure, the product was obtained as white solid (3.12g, 75% yield). **¹H NMR** (500MHz, CDCl₃) δ = 8.29 (d, *J* = 7.9 Hz, 3 H),

7.63 (d, *J* = 8.1 Hz, 3 H), 7.45 (t, *J* = 7.6 Hz, 3 H), 7.37 - 7.31 (m, 3 H), 4.99 - 4.83 (m, 6 H), 2.05 - 1.88 (m, 6 H), 1.33 - 1.18 (m, 19 H), 0.85 - 0.75 (m, 9 H), **¹³C NMR** (125 MHz, CDCl₃) δ = 141.1, 138.9, 123.5, 122.7, 121.5, 119.6, 110.5, 103.2, 47.1, 31.4, 29.8, 26.4, 22.5, 13.9, **LCMS** (ESI) *m/z* calcd for C₄₂H₅₁N₃: 345.1260, [M] Found: 345.1217.

Synthesis of compound Alkylated-TAT-Br:

To a solution of TAT-Alk (1.4 g, 2.34 mmol, 1 eq.) in 40 mL CHCl₃, (372 mg, 2.09 mmol, and 0.842 eq.) of NBS in 20 mL DMF was added dropwise via a syringe at 0 °C. After addition, the reaction mixture was stirred for 1h at room temperature. The mixture was extracted with CH₂Cl₂ and the organic phase was dried over Na₂SO₄. The obtained crude product was purified by column chromatography (Hexane:DCM = 95:5 vol/vol). After evaporation of the solvent at reduced pressure, the product was obtained as a white solid (1.03g, 53% yield). **¹H NMR** (500MHz, CDCl₃) δ = 8.29 - 8.20 (m, 2 H), 8.07 (d, *J* = 8.1 Hz, 1 H), 7.71 (s, 1 H), 7.61 (t, *J* = 6.9 Hz, 2 H), 7.47 - 7.38 (m, 3 H), 7.33 (t, *J* = 7.1 Hz, 2 H), 4.93 - 4.76 (m, 6 H), 2.01 - 1.87 (m, 6 H), 1.31 - 1.18 (m, 18 H), 0.80 (br. s., 9 H), **¹³C NMR** (125 MHz, CDCl₃) δ = 142.0, 141.0, 139.1, 139.0, 138.9, 138.5, 123.5, 123.4, 123.2, 122.9, 122.7, 122.5, 122.5, 121.6, 121.5, 119.8, 119.6, 116.1, 113.4, 110.6, 110.5, 103.5, 103.1, 102.8, 47.1, 47.1, 47.0, 31.7, 31.4, 31.4, 31.4, 29.8, 29.7, 29.6, 26.3, 26.3, 22.6, 22.5, 14.0, 13.9, **LCMS** (ESI) *m/z* calcd for C₄₂H₅₀BrN₃: 675.3183, [M] Found: 675.2885.

Synthesis of compound Alkylated-TAT-3Br:

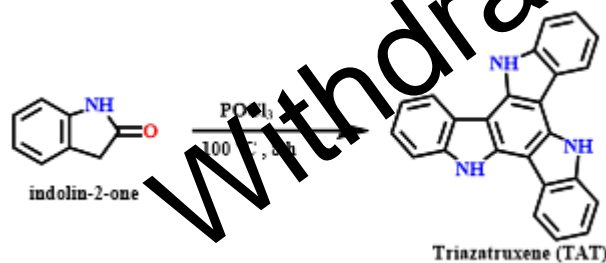
To a solution of TAT-Alk (1 g, 1.66 mmol, 1 eq.) in 90 mL CHCl₃, (915 mg, 5.15 mmol, 3.1 eq.) of NBS in 15 mL DMF was added dropwise via

a syringe at 0°C. After addition, the reaction mixture was stirred for 1h at room temperature. The mixture was extracted with CH₂Cl₂ and the organic phase was dried over Na₂SO₄. The obtained crude product was purified by column chromatography (Hexane:DCM = 95:5 vol/vol). After evaporation of the solvent at reduced pressure, the product was obtained as a pale yellow solid (1.31g, 80% yield). **¹H NMR** (500MHz, CDCl₃) δ = 7.55 (s, 3 H), 7.21 (q, J = 8.4 Hz, 6 H), 4.21 - 4.12 (m, 3 H), 4.12 - 4.01 (m, 3 H), 1.35 - 1.13 (m, 6 H), 0.67 - 0.50 (m, 9 H), 0.50 - 0.37 (m, 18 H). **¹³C NMR** (126MHz, CDCl₃) δ = 138.2, 138.0, 125.9, 123.5, 119.9, 115.2, 113.6, 107.3, 45.0, 31.2, 29.2, 25.8, 21.7, 13.8. **LCMS** (ESI) m/z calcd for C₄₂H₄₈Br₃N₃: 831.1393, [M] Found: 831.1018.

Results and discussion

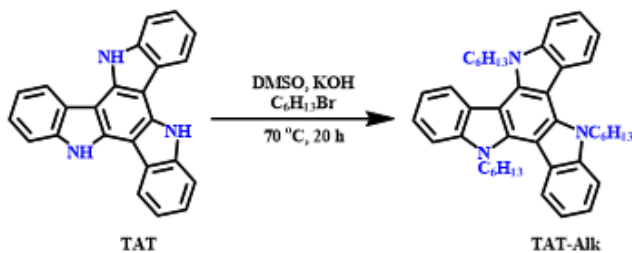
Synthetic Pathway

The symmetric cyclotrimerization of indoline-2-one in POCl₃ at 100°C, leads to the unsubstituted triazatruxene core, in 38% yield (Scheme 3) together with other open oligomers and cyclic tetramer as secondary products. The obtained product TAT was recrystallized with acetone.



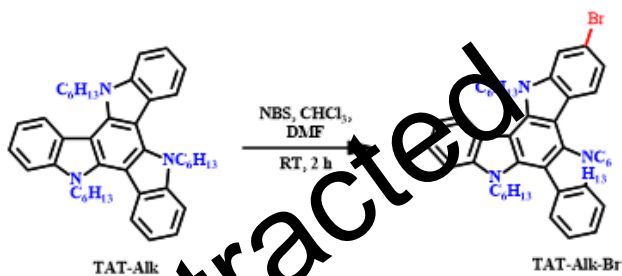
Scheme 3 Synthetic Pathway of TAT

The alkylated triazatruxene (TAT-Alk) was synthesized by performing a nucleophilic attack of nitrogen of TAT on 1-bromohexane in presence of base KOH. The reaction was carried out at 70 °C under argon atmosphere. TAT-Alk was obtained in 75% yield.



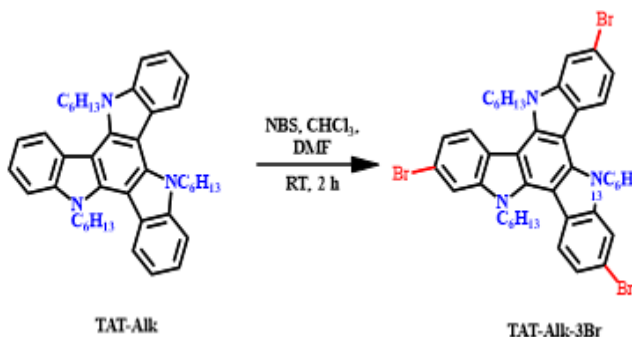
Scheme 4 Synthetic Pathway of TAT-Alk

TAT-Alk-Br was synthesized by reacting TAT-Alk with NBS (0.892 eq.) at 0°C in CHCl₃ and DMF for 2 h in 53% yield. The addition of NBS dissolved in DMF was carried out dropwise, preferentially leading to the formation of mono-brominated product.



Scheme 5 Synthetic Pathway of TAT-Alk-Br

TAT-Alk-3Br was synthesized by reacting TAT-Alk with NBS (3.1 eq.) at 0°C in CHCl₃ and DMF for 2 h in 80% yield. The addition of NBS dissolved in DMF was carried out dropwise, preferentially leading to the formation of tribrominated product.



Scheme 6 Synthetic Pathway of TAT-Alk-3Br

Photophysical Properties

The absorption spectra of TAT, TAT-Alk, TAT-

Alk-Br and TAT-Alk-3Br were recorded at room temperature in DCM (1×10^{-5} M).

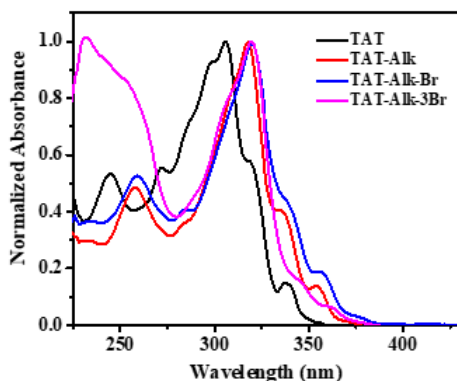


Figure 6 Normalized electronic absorption of compounds TAT, TAT-Alk, TAT-Alk-Br and TAT-Alk-3Br

The UV spectra of all the compounds displayed absorption bands between 220-380 nm. All the substituted compounds show red shifted maxima band as compared to the unsubstituted triazatruxene (TAT).

Electrochemical properties

Cyclic Voltammetry (CV)

The cyclic voltammograms of compounds TAT, TAT-Alk, TAT-Alk-Br and TAT-Alk-3Br were recorded in 0.1 M Bu_4NPF_6 in DCM at scan rate of 50 mVs^{-1} vs saturated Ag/AgCl electrode at room temperature.

All the four synthesized molecules show three oxidation waves in the anodic region showing consecutive oxidation of molecules. There is no reduction wave in the cathodic region indicating the strong donor nature of triazatruxene derivatives. In TAT, second and third oxidation wave merge to give only two oxidation waves. All the substituted molecules show anodic shift as compared to the parent triazatruxene molecule.

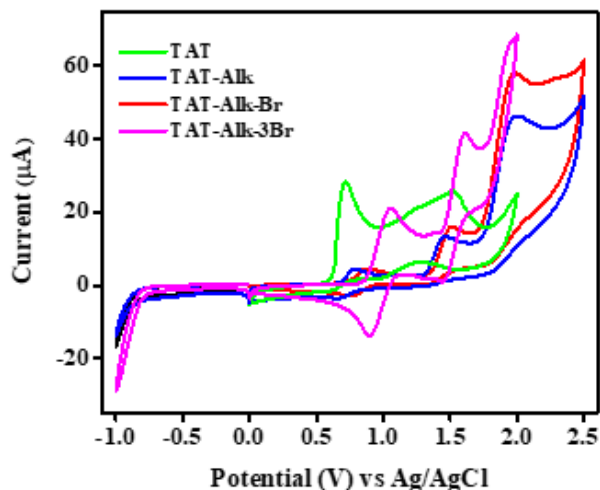


Figure 7 Cyclic voltammograms of compounds TAT, TAT-Alk, TAT-Alk-Br and TAT-Alk-3Br

Differential Pulse Voltammetry (DPV)

To further confirm the number of oxidations in anodic region, we performed differential pulse voltammograms of compounds TAT, TAT-Alk, TAT-Alk-Br and TAT-Alk-3Br in 0.1 M Bu_4NPF_6 in DCM were recorded at scan rate of 50 mVs^{-1} vs saturated Ag/AgCl electrode at room temperature. The Differential pulse voltammograms are in good correlation with the cyclic voltammograms of all the synthesized molecules.

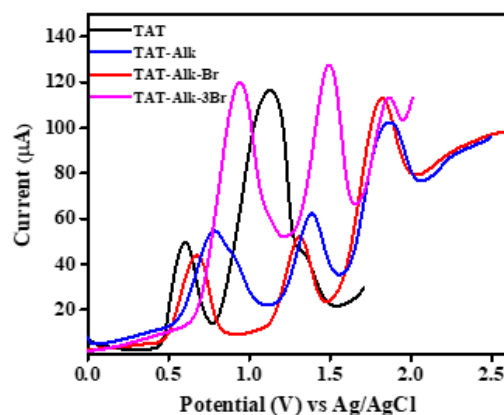


Figure 8 Differential Pulse Voltammograms of Compounds TAT, TAT-Alk, TAT-Alk-Br and TAT-Alk-3Br

Conclusion

We have synthesized three triazatruxene derivatives (TAT). These derivatives can be used as strong donors as estimated by cyclic voltammograms. These derivatives can be functionalized with various acceptor molecules leading to emitter molecules for OLEDs and HTM for solar cells.

The rising demand for energy and the quick depletion of non-renewable energy sources have led to the use of lower energy consuming electronic devices, and development of renewable energy sources like solar energy. The development of TADF OLEDs and perovskite solar cells can contribute to this energy demand. In future, there is hope for development of optoelectronic devices with increased efficiency and their commercialization for society benefits.

Acknowledgements

We extend our sincere gratitude to the Indian Institute of Technology (IIT) Indore for providing the necessary facilities and resources to carry out this research. We are also grateful to the Sophisticated Instrumentation Centre (SIC), IIT Indore, for conducting the NMR and mass spectrometry tests in a timely manner, and for the support and guidance of the faculty and staff throughout the project.

References

1. Vogel, I. (1974). Practical organic chemistry.
2. Li, X. C., Wang, C. Y., Lai, W. Y., & Huang, W. (2016). Triazatruxene-based materials for organic electronics and optoelectronics. *Journal of Materials Chemistry C*, 4(45), 10574-10587.
3. Goubard, F., & Dumur, F. (2015). Truxene: a promising scaffold for future materials. *RSC advances*, 5(5), 3521-3551.
4. Tao, L., Xie, Y., Zhao, K. X., Hu, P., Wang, B.

Q., Zhao, K., & Bai, X. Y. (2024). Triphenylene Trimeric Discotic Liquid Crystals: Synthesis, Columnar Mesophase and Photophysical Properties. *New Journal of Chemistry*.

5. Bisoyi, H. K., & Li, Q. (2014). Directing self-organized columnar nanostructures of discotic liquid crystals for device applications. In *Nanoscience with Liquid Crystals: From Self-Organized Nanostructures to Applications* (pp. 209-256). Cham: Springer International Publishing.

6. Pal, K., Raza, M. K., Legac, J., Rahman, M. A., Manzoor, S., Rosenthal, P. J., & Hoda, N. (2021). Design, synthesis, crystal structure and anti-plasmodial evaluation of tetrahydrobenzo [4, 5] thieno [2, 3-d] pyrimidine derivatives. *RSC Medicinal Chemistry*, 12(6), 970-981.

7. L. dos Santos, P., de Sa Pereira, D., Eng, J., Ward, J. S., Bryce, M. R., Penfold, T. J., & Monkman, A. P. (2013). Fine-Tuning the Photo-physics of Donor-Acceptor (D-A3) Thermally Activated Delayed Fluorescence Emitters Using Isomerisation. *ChemPhotoChem*, 7(2), e202200248.

8. Wu, T., Zhang, D., Ou, Y., Ma, H., Sun, A., Zhao, R., ... & Hua, Y. (2021). Efficient perovskite solar cells enabled by large dimensional structured hole transporting materials. *Journal of Materials Chemistry A*, 9(3), 1663-1668.

9. Ginnari-Satriani, L., Casagrande, V., Bianco, A., Ortaggi, G., & Franceschin, M. (2009). A hydrophilic three side-chained triazatruxene as a new strong and selective G-quadruplex ligand. *Organic & Biomolecular Chemistry*, 7(12), 2513-2516.

10. Pathak, S. K., Liu, H., Zhou, C., Xie, G., & Yang, C. (2021). Triazatruxene based star-shaped thermally activated delayed fluorescence emitters: modulating the performance of

solution-processed non-doped OLEDs via side-group engineering. *Journal of Materials Chemistry C*, 9(23), 7363-7373.

11. Aslan, M., Taskesenligil, Y., Piravadılı, S., & Saracoglu, N. (2021). Functionalization at non-peripheral positions of triazatruxene: modular construction of 1, 6, 11-triarylated-triazatruxenes for potentially organic electronics and optoelectronics. *The Journal of Organic Chemistry*, 87(8), 5037-5050.

12. Liu, Y., Wu, Y., Wang, T., Wang, Q., Han, X., Wu, X., & Wang, L. (2023). Bridged triazatruxene-based host materials for solution-processed thermally activated delayed fluorescence organic light emitting diodes with high power efficiency. *Organic Electronics*, 113, 106720.

13. Ahn, D. H., Kim, S. W., Lee, H., Ko, I. J., Karthik, D., Lee, J. Y., & Kwon, J. H. (2019). Highly efficient blue thermally activated delayed fluorescence emitters based on symmetrical and rigid oxygen-bridged boron acceptors. *Nature Photonics*, 13(8), 540-546.

14. Peng, X., Qiu, W., Li, W., Li, M., Xie, W., Li, W., & Su, S. J. (2022). Synergetic Horizontal Dipole Orientation Induction for Highly Efficient and Spectral Stable Thermally Activated Delayed Fluorescence White Organic Light-Emitting Diodes. *Advanced Functional Materials*, 32(28), 2201024.

Cite this article as

Tripathi S, Yadav K, Gour VN. Synthesis of Triazatruxene-based derivatives for optoelectronic applications. *J Pharmacol Biomed.* 2024; 8(4): 723-731